



Article

---

# The Hidden Dimension of Façades: Fractal Analysis Reveals Composition Rules in Classical and Renaissance Architecture

---

Vilmos Katona

## Special Issue

From Fractal Geometry to Visual Intelligence in Architecture

Edited by

Dr. Wolfgang E. Lorenz and Dr. Matthias Kulcke





## Article

# The Hidden Dimension of Façades: Fractal Analysis Reveals Composition Rules in Classical and Renaissance Architecture

Vilmos Katona

Institute of Architecture, Faculty of Engineering and Information Technology, University of Pécs,  
HU-7624 Pécs, Hungary; katona.vilmos@mik.pte.hu

**Abstract:** This study uses fractal analysis to measure the detailed intensity of well-known Classical and Renaissance façades. The study develops a method to understand their interrelated design principles more comprehensively. With this evaluation tool, one can observe intrinsic connections that support the historical continuity and point out balancing composition protocols, such as the ‘compensation rule’, that regulated design for centuries. The calculations offer mathematical constants to identify Classical and Renaissance details by plasticity rates. Finally, we base this method on spatial evaluation. Our calculations involve depth, which connects planar front views with the haptic reality of the façades’ tectonic layers. The article also discusses the cultural and urban implications of our results.

**Keywords:** fractal analysis; Hausdorff dimension; relief method; complexity; Classical architecture; Renaissance architecture; tectonic culture



**Citation:** Katona, V. The Hidden Dimension of Façades: Fractal Analysis Reveals Composition Rules in Classical and Renaissance Architecture. *Fractal Fract.* **2023**, *7*, 257. <https://doi.org/10.3390/fractalfract7030257>

Academic Editors: Wolfgang E. Lorenz and Matthias Kulcke

Received: 19 February 2023

Revised: 6 March 2023

Accepted: 8 March 2023

Published: 11 March 2023



**Copyright:** © 2023 by the author. Licensee MDPI, Basel, Switzerland. This article is an open access article distributed under the terms and conditions of the Creative Commons Attribution (CC BY) license (<https://creativecommons.org/licenses/by/4.0/>).

## 1. Introduction

This article examines historical façades with the extended analytical tool of the ‘relief method’ [1]. With this method, we seek to achieve the following goals: (1) scrutinizing the plasticity of Classical form; (2) extending knowledge on the Classical concept of tectonic balance; (3) confirming the historical integrity of Classical and Renaissance architectures; and (4) contributing mathematical constants to the understanding of Classical and Renaissance façade composition. Based on these aims, we would also like to promote the recognition of fractal analysis in architecture and cultural heritage protection.

Fractal analysis became more popular in architecture after its inception, which suggests that design methodology is today more open to applied sciences. Creating functional plans was once inalienable from the exclusive domain of architects, and the appropriateness of their products was based on isolated professional decisions. Architects nowadays use more information-based analyses and should rely on users’ feedback on existing buildings [2].

There are parallel developments in the fields of such things as space syntax, pattern languages, and visual data processing that are capable of providing a more comprehensive evaluation on design ideals and their outcomes. These evaluations are aimed primarily at supporting the three terrains of architecture: the functional, the aesthetical, and the socioeconomical. Among these, fractal analyses focus primarily on the aesthetic quality of our built environment.

Architecture has been a subject for a multitude of fractal experiments. Michael Batty and Paul Longley [3] were the first to introduce Benoit Mandelbrot’s ‘box-counting method’ to urban sciences, after which Carl Bovill [4] extended the field of its possible applications to architecture. As Wolfgang Lorenz [5], Nikos Salingaros [6], and Michael Ostwald [7,8] added newer aspects to this subject, ‘fractal aesthetics’ was soon born to gauge the complexity of human living space. These efforts were all based on the need for increasing the level of visual connectivity between urban and natural landscapes, which implicitly subsidizes the desire to develop environmental awareness.

In a more recent article on architecture, Lorenz [9] reconciled metallic proportions with Hausdorff dimensions in order to decide if the code of beauty exists in the logarithmic formulas, as previously suggested by other scholars of fractal aesthetics [10–12]. In their calculations, though, they analyzed planar images (i.e., projections) of the buildings' frontages, or intentionally pixelated architectural drawings. Consequently, the resulting dimensions ( $D_H$ ) were expected to fall below 2. Not even Salingaros [13] argues about the validity of this kind of planar evaluation; however, he has been consistently replacing geometrical proportion with scaling proportion, claiming that the latter does enhance complexity, while the effect of the former has no supporting evidence.

Because these computations did not involve depth, we introduced the 'relief method' [1], which we considered as a possible way to capture the haptic nature of architecture beyond the apparent two-dimensionality of elevations. By recognizing the self-similar patterns in the façades' tectonic layers [14,15], we could identify the epoch and the place where a certain edifice was constructed. In other words, we attempted to reveal the arithmetical essence of the façades of well-known historical buildings. We believed that these patterns were reflections of *genius loci* [16,17]. A similar method can be used for a more specific survey on Classical details.

When studying these details, we must distinguish between the architecture of Classical antiquity and the Renaissance. Relative to Classical antiquity, the character of Renaissance edifices changed from freestanding compositions to dense urban collages, which were less three-dimensional but visually more individual; this was possible compensation for the loss of space around the joint elevations looking down onto populated main streets [17] (pp. 138–165).

This also implies that the sculptural architectural components, such as the columns, disappeared or were compressed into relief layers [15] as part of the urban 'scenes'. These were dominated by walls, not by pillars and beams as in the time of the ancient fora, but similar details were added to them as reliefs. Entablatures were replaced by cornices that no longer rested on columns. However, the old construction logic prevailed in the trabeated systems of porticoes, wall cornices, window jambs, and lintels.

## 2. Definitions and Principles

We focus on analysis of architectural elevations, and continuing our latest investigations [1], we point out the novelties and implications of our approach, which we apply this time specifically to Classical architecture. For this purpose, we need to define our principles and work methods.

First, by Classical architecture, we mean the Vitruvian way of building [18], specifically the architecture of the ancient Greco-Roman world together with its codification and formal interpretations by Renaissance theory and praxis. The drawings were therefore collected from multiple Renaissance sources for graphic analysis, the purpose of which was to extract numerical data for plasticity evaluations.

The term 'plasticity' is another keyword that describes the focus of our investigation. Though fractal computations usually consider façades as two-dimensional images—for example, for box-counting the 'black voids' inside the building's contour—we integrate depth as a crucial parameter in our calculations [1]. This means that we consider façades as tectonic reliefs [14]. These reliefs are almost but not quite planar, since their function is to 'compress' and partly reveal information about the hidden structure of the building [19–22].

Yet another important feature of Classical architecture is that its design tools were planar, which created certain tensions between the two-dimensional plans and the realized buildings. Our plasticity measurement is partly designed to resolve this tension (see the description of the calculation method), for which we need to find out how to construe the elevation's structural layers.

The vertical base plane always has to be perpendicular to the shortest Euclidean line between the façade and the observer. This does not need any clarification in the case of Renaissance urban palazzos, where windows plausibly define the base planes of the

elevations. However, when examining a Doric temple from the seventh century BCE, the whereabouts of this plane is less obvious. If we measure its colonnade, the plane cuts through the columns in the middle; that is, the plane contains the central axes of all the shafts. The same applies to the pillars and porticoes of other edifices.

However, given the fact that frontage compositions often integrate freestanding details, we need to consider visibility. When freestanding details, such as a set of smaller columns, cover a certain region of the background wall—a very common phenomenon in Palladian motifs [23]—the base plane jumps to the fore to cut the elements in half. Meanwhile, the plane does not break if the same columns are attached to the wall in such a way that only a part of them remains (Figure 1).

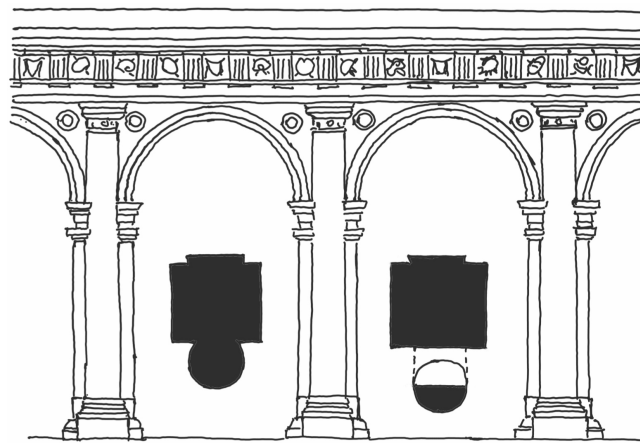


**Figure 1.** A segment of the façade of Palazzo Farnese, Rome (Antonio da Sangallo Jr., 1534), showing the true horizontal section of its pillars (**left**) and a virtual case when columns are freestanding (**right**). According to our methodological considerations, the tangible front contour of the former is longer than that of the latter.

The latter implies that some columns' surface area may be hidden from sight due to its round shape, but it will nonetheless appear in our calculations. This means that some highly sculptural parts of the tectonic relief may increase the elevation's overall plasticity more intensely than freestanding components. It is also very easy to foresee that pilasters, being the flattened transformations of the columns, will lose their three-dimensional and tactile value compared with their round relatives [24].

Another important principle of our fractal evaluation is based on the observation that Classical architecture is composed of perpendicular pieces, the surfaces of which are essentially 'extruded contours'. In other words, both posts and lintels of any scale have two definitive sections: one that reveals the plastic contour and another one that is theoretically rectangular. Thus, to measure the areal plasticity of a tectonic object relative to its two-dimensional 'flat projection', it is possible to compare its undulating contour with a straight line (Figure 2).

This comparison, though, is more complex than a mathematical proportion [25], assuming that Classical buildings, like any kind of material structure or living organism, are composed of quasi-self-similar patterns [26]: the closer we look, the more vibrant details we discover. Not only do ornaments make us feel Classical architecture's closeness to nature, but their details also hide or reveal themselves due to the observed scale [27]. In praxis, plans are traditionally abstracted or enhanced due to scale, which is also a rather simple skill to learn in design education.

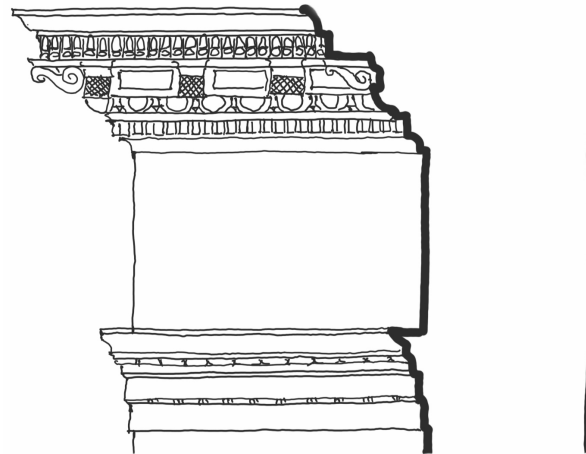


**Figure 2.** The cornicione (top wall cornice) of Palazzo del Magnifico in Siena (Giacomo Cozzarelli, ca. 1500). Fractal dimensions are calculated by comparing the length of the curvilinear section contour (left) with the length of the same contour's visible span (right).

Quasi-self-similarity, on the other hand, dictates that we can only work with a limited number of scaling layers on the façade, and, most importantly, that we cannot magnify buildings further than the ornamental level without stepping into the realm of material science. However, we cannot exclude the fact that material textures could also result in similar constant values as built structures and substructures. The constants hereby used and investigated are derived from the Hausdorff–Besicovitch formula, which describes fractal dimensions with a single number,  $D_H$ .

We expect that by calculating the Hausdorff dimensions in a multitude of Classical details, we can extract crucial information about the visual complexity as well as the covert proportional integrity of these historical buildings.

### 3. Methodological Considerations on Scale

#### 3.1. The Vitruvian Module

Scale-Sensitive Fractal Analysis (SSFA) is used in surface morphology as an application of Mandelbrot's topographical theorem [26] in different fields of design and engineering. This has relevance here, as depth and the relative surface ratio seem to be the common ground for SSFA's area-scale method [28,29] and our own relief method [1]. The former's implication that the reference scale affects the fractal dimension foreshadows a similar scale problem in our plasticity measurement. The dilemma is of profound mathematical nature, which we can illustrate with an example of the Sierpiński carpet and its architectural equivalent.

It is well understood that the Hausdorff dimension of the carpet is  $\log 8 / \log 3 \approx 1.893$ . This value results from the logarithmic comparison of the square's side length ( $a$ ) with the remnant area ( $A$ ) encompassed by the square's perimeter, provided that this base pattern self-similarly repeats itself on every scale. However axiomatic it looks, though, the calculation that places the pattern into a 3-by-3 grid is more of a convention (Figure 3).

We are free to draw a different grid without changing the geometry (e.g., 30-by-30), in which case  $D_H = \log 800 / \log 30 \approx 1.965$ . The latter is closer to 2 than the former calculated value, because whatever area and length we choose, with  $n$  as a grid multiplier we arrive at the following limit:

$$\lim_{n \rightarrow \infty} \frac{\log An^2}{\log an} = 2 \quad (1)$$

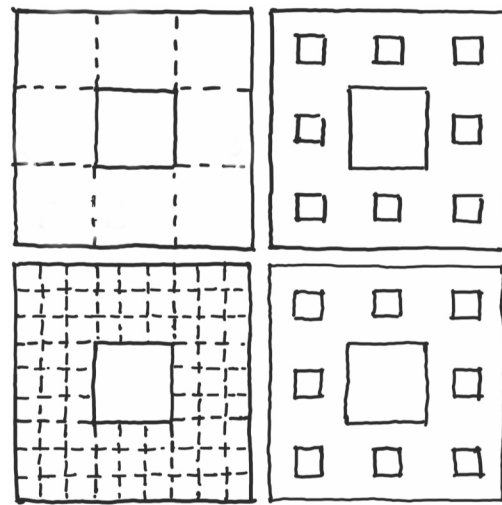


**Figure 3.** Two grid variations for the same Sierpiński carpet. Changing the grid/resolution (first column) does not change the fractal pattern (second column) but does affect the dimension.

This means that the thicker the grid we define, the closer we reach two-dimensionality with the possible grid variations of the Sierpiński pattern. The same would apply to an imaginable elevation inspired by the fractal carpet. The result for the Hausdorff dimension would differ depending on our decision to measure it in feet or in inches. Moreover, when analyzing drawings or images, the digital resolution [9] and even the size of our computer screen may influence the conclusion. At this point, we need to reconsider our concept of scale regarding either a plan or a physical building. The logic of Classical architecture is about to help.

When describing his trifold doctrine (*firmitas*, *utilitas*, *venustas*) on architecture, Vitruvius [18] also phrased his views on order and symmetry [30]. His attention, as perhaps that of any architect in the Mediterranean in his day, was not primarily focused on the buildings' actual sizes but rather on their compound geometrical proportions, which were widely believed to be responsible for beauty [31]. The latter's integrity was deeply instilled in that no external unit of measure was allowed to rule over the planning.

The Roman modulus—otherwise known as the Vitruvian module—was, though, a common denominator that established a self-referential unit for the edifice. This module corresponded to the radius of one of the building's columns at its base [18] (Book IV, Chapter III.3). Regarding the scale, it meant that the building itself had to contain the unit with which its own size could be measured.

This way of thinking has not theoretically changed ever since that time. Even Peter Eisenman acknowledged the validity of self-referential planning [32], based on Le Corbusier's Dom-Ino House, despite claiming that deconstructivism has surmounted the so-called Classical paradigm. Modularity is an innate feature of Classical design—and perhaps of every design—so making the Vitruvian module our scaling unit for logarithmic dimensions seems less arbitrary than using any other possible method.

### 3.2. The Significance of $\pi$

After setting the Vitruvian module as the referential unit, we are able to find some rather intriguing results regarding the Classical orders' system of proportions. It is not difficult to calculate the visible perimeter of circle-based columns, which equals  $\pi$  if the diameter of the column is exactly 2. If we write these values into the linear Hausmann equation, as if we wanted to measure the plasticity of the column's curvature relative to a line, then we obtain the following result:

$$\frac{\log \pi}{\log 2} \approx 1.651 \quad (2)$$



This value is rather close to  $\phi$  (i.e., the golden ratio), which is one of the principal numbers of the proportional systems used to create the buildings and designs of Classical antiquity, the others being derived from  $\sqrt{2}$  or  $\sqrt{3}$  [33]. For curiosity's sake, let us add that a logarithmic comparison between the diameter and the full perimeter of the column would result in a value significantly close to both another recurrent Classical proportion,  $1 + \sqrt{3}$  [34], and  $e$  (Euler's number):

$$\frac{\log 2\pi}{\log 2} \approx 2.651 \quad (3)$$

Moreover, if we compare the Greek and Roman variants of the Classical orders [35] (pp. 37–38), we find that the average ratio of the heights of an ideal entablature and its frieze is nearly  $\pi$  (Table 1).

**Table 1.** Height ratios of entablatures and friezes listed by typical variants of the Classical orders.

Category	Type	Height of Entablature [mod] <sup>2</sup>	Height of Frieze [mod]	Ratio	Average Ratio
Greek	Doric	4.000	1.500	2.667	3.254
	Ionic (Attica) <sup>1</sup>	4.500	1.667	2.700	
	Ionic (Asia Minor)	5.500	1.000	5.500	
	Corinthian (Andronicus)	3.667	0.833	4.400	
	Corinthian (Lysicrates)	5.000	1.500	3.333	
Roman	Tuscan	3.500	1.167	3.000	3.254
	Doric (with dentils)	4.000	1.500	2.667	
	Doric (with consoles)	4.000	1.500	2.667	
	Doric (Albano)	3.667	1.500	2.444	
	Ionic	4.500	1.500	3.000	
	Corinthian	5.000	1.500	3.333	
	Composite	5.000	1.500	3.333	

<sup>1</sup> Subvariants indicated in parentheses are distributed from György Kardos [35] (pp. 37–38). <sup>2</sup> The unit of measure is the Vitruvian module (ibid.).

Occupying the middle, a frieze is a distinguished part of the entablature. It is often a plain ribbon that hosts figural reliefs, which is in contrast with the rest of the horizontal entity, namely the architrave and the cornice. These two are of plastic character, and whatever ornaments they host, those are more organic part of them than the added motifs that usually populate the frieze (Figure 4).

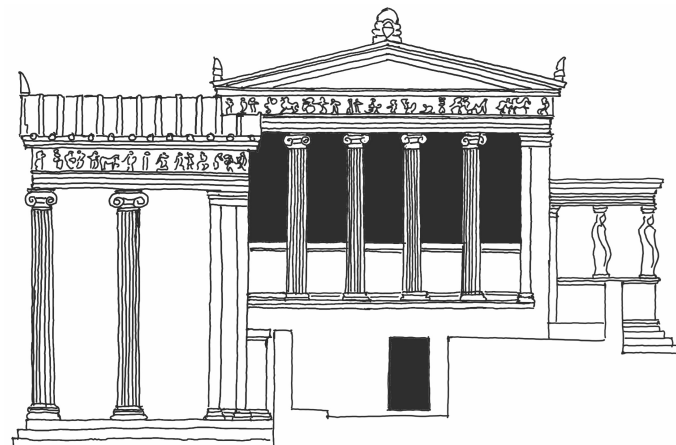


**Figure 4.** A reconstruction of the west elevation of the Erechtheion in Athens, illustrating the frieze as the most richly detailed part of the entablature.

From this also follows that the entablature's section implies an abstract segment—a line—that is offered as an alternative referential unit for calculating the fractal dimension of the cornice's complete profile. These considerations suggest that we should put the entablature's height as  $\pi$  times the referential unit so that all the other parts could be measured relative to it before the logarithmic plasticity evaluation takes place.

Finally, we apply the same mathematical notation to the entablature as we applied to the columns, but in this case we divide its height, not the perimeter, by  $\pi$  when defining its referential unit. As a pragmatic argument, this notation results in normalized Hausdorff dimensions by which we avoid extraordinary results from the  $f(x)$  logarithmic functions when  $x \approx 1$  or  $x < 1$ . Another benefit of this method is that it simplifies our calculations both in general and with special regard to the Feret diameter.

### 3.3. Involving the Feret Diameter

As a part of our methodological overview, the methodological problem of logarithmic scale and its solution leads quickly to another question: How do we measure the size of a Classical detail? In Paestum, Italy, for instance, the archaic columns of Poseidon's Doric temple are robust; the fluted shafts are only about four times as high as their base diameters [35] (pp. 37–38). The chunky proportions are partly due to the *entasis*, which make columns curve slightly because their diameters are decreased from the bottom upward.

Consequently, when the shaft arrives at the capital, its diameter reduces by a third. It would be most difficult to describe the size of such a column with only one mathematical variant. For simplification, we may choose between the horizontal and the vertical dimensions and put either of them as the 'size' of the column.

This seems obvious for the orthogonal character of the Classical façade, but if we fathom the column's scale like that, we overlook its curvature. Less symmetrical parts would also be hard to handle in this way. We could, of course, measure an object similarly along any specified direction, yet none of the results would be complete. Instead, we take one component's Feret diameter ( $F$ ) averaged over all directions. It follows from Cauchy's theorem [36] that for a two-dimensional convex body, this averaged value equals the ratio of the object's perimeter ( $P$ ) and  $\pi$ , that is,  $F = P/\pi$ .

Although Feret diameter is used mostly for measuring the size of microscopic particles, it proves useful in the current analysis as well. Tables 2–8 show information on the averaged Feret diameter on a modular basis and sort objects by scale regardless of their actual size. The comparisons between the types of architectural elements shed light on some general proportions that characterize the buildup of a Classical edifice.

**Table 2.** The calculated geometric parameters of Classical shafts leading to the average values of Feret diameter and Hausdorff dimensions.

Type	Location/Source	Rel. * Contour ( $c$ )	Rel. * Length ( $l$ )	Feret Diameter ( $F$ )	Linear Fract. Dim. ( $D_{H1}$ )	Areal Fract. Dim. ( $D_{H2}$ )
Greek Doric	Parthenon, Athens	3.380	10.732	8.106	1.757	2.342
Greek Ionic (Attica)	Erechtheion, Athens	4.548	17.041	12.122	2.185	2.466
Greek Ionic (Asia Minor)	Temple of Athena Polias, Priene	4.469	17.778	12.591	2.160	2.450
Greek Corinthian	Choragic Monument of Lysicrates, Athens	4.732	16.423	11.728	2.243	2.493
Greek Corinthian	Horologion of Andronicus, Athens	4.615	15.154	10.920	2.206	2.490
Tuscan	After S. Serlio	3.147	12.147	9.006	1.654	2.284
Roman Doric	Theatre of Marcellus, Rome	3.147	16.206	11.590	1.654	2.261
Roman Ionic	After V. Scamozzi	3.147	16.559	11.815	1.654	2.259
Roman Corinthian	Temple of Antonius and Faustina, Rome	3.147	16.706	11.909	1.654	2.258
Composite	Baths of Diocletian, Rome	3.147	16.853	12.002	1.654	2.258
			Average:	11.179	1.882	2.356

\* Measures of section contours and sample lengths are relative to the reference unit  $s_0/2$ .



**Table 3.** The calculated geometric parameters of Classical entablatures leading to the average values of Feret diameter and Hausdorff dimensions.

Type	Location/Source	Rel. * Contour (c)	Rel. * Length (l)	Feret Diameter (F)	Linear Fract. Dim. ( $D_{H1}$ )	Areal Fract. Dim. ( $D_{H2}$ )
Greek Doric	Parthenon, Athens	4.324	29.174	20.573	1.279	2.141
Greek Ionic (Attica)	Erechtheion, Athens	4.333	19.825	14.621	1.281	2.156
Greek Ionic (Asia Minor)	Temple of Athena Polias, Priene	4.789	23.179	16.756	1.368	2.197
Greek Corinthian	Horologion of Andronicus, Athens	5.434	11.038	9.027	1.479	2.309
Tuscan	After G. B. da Vignola	4.528	9.887	8.294	1.319	2.213
Roman Doric	Theatre of Marcellus, Rome	5.934	340.468	218.749	1.556	2.182
Roman Ionic	Fortuna Virilis, Rome	4.460	14.513	11.239	1.306	2.183
Roman Corinthian	Pantheon, Rome	4.466	34.080	23.696	1.307	2.151
Composite	Arch of Titus, Rome	4.747	25.216	18.053	1.361	2.189
Composite	Arch of Septimius Severus, Rome	4.667	36.536	25.260	1.346	2.167
			Average:	36.627	1.360	2.189

\* Measures of section contours and sample lengths are relative to the reference unit  $s_0/\pi$ .**Table 4.** The calculated geometric parameters of Classical capitals leading to the average values of Feret diameter and Hausdorff dimensions.

Type	Location/Source	Rel. * Contour (c)	Rel. * Length (l)	Feret Diameter (F)	Linear Fract. Dim. ( $D_{H1}$ )	Areal Fract. Dim. ( $D_{H2}$ )
Greek Doric	Temple of Poseidon, Paestum	4.552	3.847	4.449	1.324	2.298
Greek Ionic (Attica)	Propylaea, Eleusis	5.701	4.305	4.741	1.521	2.458
Greek Ionic (Asia Minor)	Temple of Athena Polias, Priene	6.761	5.259	5.348	1.670	2.547
Greek Corinthian	Choragic Monument of Lysicrates, Athens	6.359	1.925	3.226	1.616	2.784
Greek Corinthian	Temple of Olympian Zeus, Athens	5.462	2.236	3.423	1.483	2.568
Tuscan	After S. Serlio	3.867	4.108	4.615	1.181	2.162
Roman Doric	After A. Palladio	4.833	4.773	5.038	1.376	2.318
Roman Ionic	Baths of Diocletian, Rome	5.576	7.069	6.500	1.501	2.370
Roman Corinthian	Temple of Castor and Pollux, Rome	7.038	2.326	3.481	1.705	2.811
Composite	Temple of Vesta, Tivoli	7.906	2.727	3.736	1.806	2.859
			Average:	4.456	1.518	2.517

\* Measures of section contours and sample lengths are relative to the reference unit  $s_0/\pi$ .**Table 5.** The calculated geometric parameters of Renaissance jambs leading to the average values of Feret diameter and Hausdorff dimensions.

Year of Construction	Location and Architect	Rel. * Contour (c)	Rel. * Length (l)	Feret Diameter (F)	Linear Fract. Dim. ( $D_{H1}$ )	Areal Fract. Dim. ( $D_{H2}$ )
1460	Pal. Piccolomini, Pienza (B. Rossellino)	3.961	11.337	9.217	1.202	2.130
1465	Pal. Ducale, Urbino (L. da Laurana)	4.326	16.171	12.295	1.279	2.163
1470	S. Giobbe, Venice (P. Lombardo)	4.398	11.355	9.229	1.294	2.188
1483	Pal. Fava, Bologna (G. Montanari)	4.435	9.583	8.101	1.301	2.203
1486	Pal. Cancellaria, Rome (D. Bramante)	4.575	19.897	14.667	1.328	2.182
1489	Pal. Strozzi, Florence (B. da Maiano)	5.041	17.461	13.116	1.413	2.236
1560	Loggia dei Branchi, Bologna (G. da Vignola)	4.374	19.327	14.304	1.289	2.161
1564	Pal. Negroni, Rome (B. Ammanati)	4.099	22.560	16.362	1.232	2.125
1586	Pal. Laterano, Rome (D. Fontana)	4.264	10.238	8.518	1.267	2.176
1739	Pal. della Consulta, Rome (F. Fuga)	4.528	13.583	10.647	1.319	2.195
			Average:	11.646	1.293	2.176

\* Measures of section contours and sample lengths are relative to the reference unit  $s_0/\pi$ .**Table 6.** The calculated geometric parameters of Renaissance lintels leading to the average values of Feret diameter and Hausdorff dimensions.

Year of Construction	Location and Architect	Rel. * Contour (c)	Rel. * Length (l)	Feret Diameter (F)	Linear Fract. Dim. ( $D_{H1}$ )	Areal Fract. Dim. ( $D_{H2}$ )
1447	S. Spirito Sagrestia, Florence (A. di Lazzaro Cavalcanti)	4.635	6.283	6.000	1.340	2.261
1450	Casa Sanmicheli, Verona (M. Sanmicheli)	4.752	3.888	4.475	1.361	2.331
1460	Pienza Cathedral (B. Rossellino)	4.315	5.223	5.325	1.277	2.227
1475	Pal. Ducale, Gubbio (L. da Laurana)	4.131	5.853	5.726	1.239	2.188
1489	S. Spirito Sagrestia, Florence (G. da Sangallo)	4.476	7.058	6.493	1.309	2.228
1501	Pal. Cenami, Lucca (F. Marti)	4.107	5.879	5.743	1.234	2.184
1534	Pal. Farnese, Rome (A. da Sangallo Jr.)	6.126	4.608	4.933	1.583	2.500
1541	Pal. Venezia, Rome (J. da Pierasanta)	4.098	7.103	6.522	1.232	2.171
1545	Turini Chapel, Pescia Cathedral (G. di Baccio d'Agnolo)	4.697	4.518	4.876	1.351	2.303
1586	Pal. Laterano, Rome (D. Fontana)	3.927	10.001	8.367	1.195	2.129
			Average:	5.846	1.312	2.252

\* Measures of section contours and sample lengths are relative to the reference unit  $s_0/\pi$ .

**Table 7.** The calculated geometric parameters of Renaissance porticoes leading to the average values of Feret diameter and Hausdorff dimensions.

Year of Construction	Location and Architect	Rel. * Contour ( <i>c</i> )	Rel. * Length ( <i>l</i> )	Feret Diameter ( <i>F</i> )	Linear Fract. Dim. ( <i>D<sub>H1</sub></i> )	Areal Fract. Dim. ( <i>D<sub>H2</sub></i> )
1510	Pal. Apostolico, Loreto (D. Bramante)	4.006	4.555	4.900	1.212	2.183
1524	Pal. Giustiniani, Padua (G. M. Falconetto)	5.122	4.029	4.565	1.427	2.385
1534	Pal. Farnese, Rome (A. da Sangallo Jr.)	6.113	7.896	7.027	1.582	2.415
1536	Libreria, Venice (J. Sansovino)	5.850	5.525	5.517	1.543	2.436
1541	Pal. Venezia, Rome (J. da Piertasanta)	5.672	6.109	5.889	1.516	2.400
1549	Basilica, Vicenza (A. Palladio)	5.341	4.712	5.000	1.464	2.394
1564	Pal. Negroni, Rome (B. Ammanati)	3.566	9.000	7.730	1.111	2.076
1589	Cancellaria, Rome (D. Fontana)	4.638	2.917	3.857	1.340	2.352
1616	Pal. Sciarra, Rome (A. Labacco)	4.353	3.860	4.457	1.285	2.261
1696	Pal. Montecitorio, Rome (C. Fontana)	5.818	2.327	3.481	1.538	2.619
Average:				5.242	1.402	2.352

\* Measures of section contours and sample lengths are relative to the reference unit  $s_0/\pi$ .

**Table 8.** The calculated geometric parameters of Renaissance wall cornices leading to the average values of Feret diameter and Hausdorff dimensions.

Year of Construction	Location and Architect	Rel. * Contour ( <i>c</i> )	Rel. * Length ( <i>l</i> )	Feret Diameter ( <i>F</i> )	Linear Fract. Dim. ( <i>D<sub>H1</sub></i> )	Areal Fract. Dim. ( <i>D<sub>H2</sub></i> )
1446	Pal. Rucellai, Florence (L. B. Alberti)	6.178	65.136	43.467	1.591	2.254
1451	Loggia del Consiglio, Padua (M. di Bassano)	5.079	18.692	13.900	1.420	2.236
1460	Pal. Piccolomini, Pienza (B. Rossellino)	5.393	73.985	49.100	1.472	2.198
1547	Pal. Farnese, Rome (Michelangelo)	5.969	63.281	42.286	1.561	2.243
1549	Basilica, Vicenza (A. Palladio)	4.978	16.336	12.400	1.402	2.234
1558	Loggia del Comune, Brescia (J. Sansovino)	4.805	33.929	23.600	1.371	2.182
1564	Pal. Doria-Tursi, Genoa (R. Lurago)	5.210	48.886	33.122	1.442	2.201
1586	Pal. Laterano, Rome (D. Fontana)	4.960	76.225	50.526	1.399	2.167
1662	Pal. Salviati, Rome (C. Rainaldi)	5.249	110.990	72.658	1.448	2.175
1666	Pal. Bonaparte, Rome (G. A. da Rossi)	5.174	33.338	23.224	1.436	2.215
Average:				36.428	1.454	2.210

\* Measures of section contours and sample lengths are relative to the reference unit  $s_0/\pi$ .

#### 4. The Calculation Method

We use fractal analysis in order to quantify the haptic quality of tectonic reliefs. For the plasticity evaluation, we extract numerical data from the drawings (i.e., sections), ground plans, frontage views, and miscellaneous details published in multiple Renaissance treatises [23,37–40]. From this collection of plans, we choose examples from a wide range of well-known Classical buildings.

Our calculations are aimed at providing single constants that describe the plasticity of the most characteristic parts of an elevation from either the Renaissance or Classical antiquity. The categories follow a logic that classifies elements into the vertical group of posts and the horizontal group of lintels [41]. Posts are columns, pilasters, porticoes, and jambs, while lintels are entablatures, wall cornices (cornicioni), and lintels of doors and windows. Capitals that create a formal and structural transition between the two have a special category, but we use the same method nonetheless to measure their visual plasticity.

To display an example of how our calculations are made, we first need to introduce simple variants. When analyzing, for instance, a segment of the Parthenon's entablature, we need to measure the section's tangible contour ( $c_0$ ), its visible span ( $s_0$ ), and the sample's length ( $l_0$ ) on the drawing (Figure 5).

The latter is always perpendicular to the former two. Then, in order to make the measured values comparable with other samples, we need to scale them all down by dividing them with a specific reference unit ( $u$ ), which equals to  $s_0/\pi$ . (In case of columns' shafts, though,  $u$  would be calculated differently— $s_0/2$ —for the reasons described above in connection with the Vitruvian module.) This notion results in the relative lengths of the section contour ( $c$ ), the section span ( $s$ ) and the sample length ( $l$ ). We can finally use these relative values to calculate the Feret diameters and the Hausdorff dimensions for plasticity evaluation by category. For the Feret diameter, we use the following formula:

$$F = \frac{2}{\pi}(s + l) \quad (4)$$

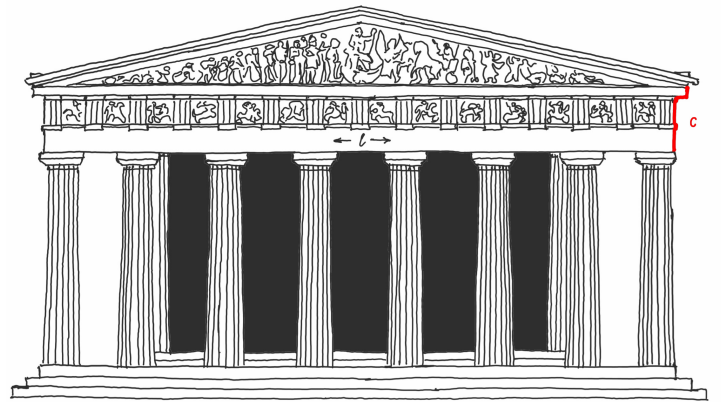


**Figure 5.** A reconstruction of the east elevation of the Parthenon in Athens, illustrating the entablature's basic variables: contour ( $c$ ), span ( $s$ ) and length ( $l$ ).

Due to some simplifications, the same values could be gained directly from architectural drawings regardless of scale except for the column's case:

$$F = 2 \left( 1 + \frac{l_0}{s_0} \right) \quad (5)$$

Finally, we apply our variables to the Hausdorff–Besicovitch formula to get the fractal dimensions of the elements. According to the linear model, the section's contour gives us the following value for the fractal dimension:

$$D_{H1} = \frac{\log c}{\log s} \quad (6)$$

Now, for the areal model relevant in plasticity measurement, we need to consider the logarithmic proportion of the plain visible area ( $A_v$ ) and the extended haptic area ( $A_h$ ) that involves depth. In other words:

$$D_{H2} = \frac{\log A_h}{\log \sqrt{A_v}} \quad (7)$$

Using our variables, this expression alters to a somewhat simpler form:

$$D_{H2} = 2 \frac{\log cl}{\log sl} \quad (8)$$

It is necessary to note here that neither the linear nor the areal fractal dimension is specified according to the area-scale method of SSFA [28,29], since we fixed the scale by a reference unit and made all the measurements relative to it. For a thorough explanation, it is also mandatory to underline that our relief method focuses on the difference between the visible and the tactile, not the approximation of the tactile; hence, the comparison is always between the visible span ( $s$ ) and the tangible contour ( $c$ ).

Herein, we analyze Classical details and not the elevation in general. We expect that the values of  $D_{H1}$  will mostly occur between 1 and 2, while those of  $D_{H2}$  will virtuously occupy the dimension gap between 2 and 3. All these calculations are intended to inform us about the plasticity of the details by the selected categories. We attempt to reveal their intrinsic connections and understand the computed values as one of the mathematical cornerstones of the Classical sense of proportion.

## 5. Values of Scale and Plasticity (Results)

### 5.1. The Fractal Dimensions of Classical Orders

As before, we follow the tectonic logic of posts and lintels when categorizing Classical details. These groups of elements do not require any novel approach and could easily be derived from the historical interpretations of the Vitruvian system [18]. Let us begin our calculations with the Classical column (Table 2) and entablature (Table 3) with the established principles.

For this, we take examples from both Hellenic and Roman antiquity, with the most characteristic types depicted by Renaissance and later scholars. The table for the shafts lists fluted and plain columns, the former being associated with the Greek variants and the latter with the Roman variants. Fluted shafts are the Doric, two alternatives of the Ionic (from Attica and from Asia Minor), and two alternatives of the Corinthian columns. Plain shafts are the Tuscan, the Roman Doric, the Ionic and Corinthian, and finally the Composite type. Fluted and plain types are represented by five examples each so that the balance between Hellenic and Roman architecture could be obtained. Each type is coupled with the source location of the analyzed sample.

The drawings' digitally measured data (relative section contour and sample length) determines the element's Feret diameter, the linear dimension, and the areal fractal dimension, given that the relative section span ( $s$ ) is exactly two modules wide. All the other values are relative to the chosen module nonetheless. We consider average values of Feret diameters and Hausdorff dimensions as the constants of Classical plasticity. For clarity, we present the results below and endeavor to interpret them afterwards.

The general increase in plasticity from the modest Doric or Tuscan to the most decorative Corinthian or Composite is not surprising; however, it is worth noting that columns have different values than entablatures. The latter's plasticity seems to be reduced relative to that of the shafts, especially if they are fluted. The verticality of the columns are naturally more stressed, yet this is only true for the abstract building, since these calculations are based on the relief sections that exclude any painted ornaments.

If we look at the reconstructions of Classical entablatures' figurative imagery [42,43], we cannot ignore the richness of painted details that are concentrated on the entablatures—respectively on the friezes—to compensate for this slight loss of plasticity. This implies that the builders of these Classical temples must have chosen to balance the façades' level of ornamentation, that is, the visual attractiveness with both plastic and planar means. In other words, they attempted to keep the fractal dimension of the buildings' 'membranes' [19] as homogenous as possible. This rule seems to apply when comparing the same types of elements of different magnitudes.

There is yet another intriguing tendency to interpret, which is more difficult to notice for the first time. Up to this point, it was less of a tiring quest to determine the length of a Classical public building's entablature. Whenever possible, we chose samples that were best offered by the well-known front elevations or their representative entrances.

The Feret diameters inform us about the proportions of these details, which do not seem to vary too much due to the Vitruvian logic of proportions [30]. However, at the sunset of the ancient Roman Republic, the appearance of centralized power manifested itself through new architectural means [44], as in the case of the Theatre of Marcellus (see Table 3), the remains and reconstruction [45,46] of which were also subject to our investigations.

The theatre, formally inaugurated in 12 BCE by Caesar Augustus, was a prestigious public edifice in Rome that was designed to represent imperial peace and unity (Figure 6).

The structure's entablatures resting on vaulted porticoes were therefore obviously undivided and encompassed the round shaped building like horizontal belts. No wonder, as their relative lengths together with their Feret diameters are exceedingly high. This example is very useful, though, because it shows how the plasticity indicator of the Hausdorff dimension remains relatively stable despite the increased length. This is unambiguously

due to the growth of the section contour's length, which triggers a sort of overcompensation in the linear fractal dimension.

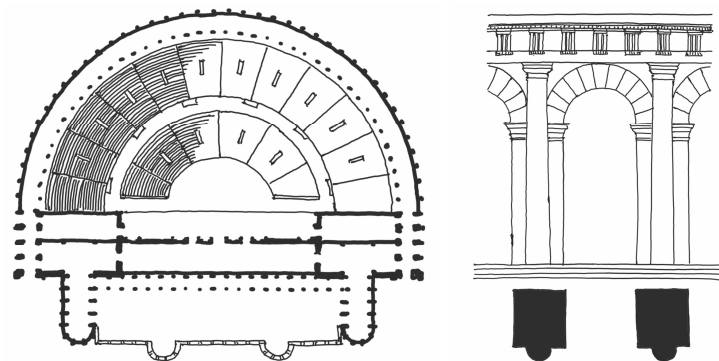


**Figure 6.** Simplified ground plan (**left**) and a segment of the round façade (**right**) of the ancient Theatre of Marcellus in Rome (reconstruction after Alberto Calza Bini [45]).

To keep the areal dimension of a long entablature on a certain level, one must certainly increase the complexity of its pattern. The logarithmic formula suggests the appropriate proportion for this notion in either Classical antiquity or Renaissance architecture. Before examining the latter, let us test the haptic features of the Classical capitals (Table 4).

For better understanding, it needs to be emphasized that the capitals' plasticity is calculated from the contours of their vertical sections; therefore, the logarithmic reference unit is derived not from the Vitruvian module but instead from the capital's height divided by  $\pi$ , as in the case of the entablatures.

This approach was inspired mostly by the Ionic capital that often captures the viewer with the planar composition of its volutes, which differs from the shaft's circular symmetry and modular order. Because of this inherent two-dimensionality, the capital is more similar to the entablature in nature, although it has a role of connecting the vertical and horizontal parts.

The increase in the areal Hausdorff dimension signifies the capital's high plasticity, as one could have envisaged, for this is usually the most densely detailed part of the column. Its linear dimension, though, is between that of the shaft and the entablature. This is a coherent result, since the capital has to bridge the intensity gap between the shaft and the sculptural trifold structure of the architrave, frieze, and cornice. On the other hand, the contour of its vertical section should not differ too much from the contour of the entablature, since together they create a continuous curve.

## 5.2. The Fractal Dimensions of Renaissance Façades

As mentioned before, one of the goals of this article is to find mathematical evidence for the continuity of Classical aesthetics in Renaissance architecture, for which we analyze the tectonic patterns of mostly Italian urban palaces. Nonetheless, beyond these outstanding historical masterpieces of the Quattrocento and Cinquecento, we will examine some younger examples and extend our investigation to as far as the 18th century.

One could aptly ask how much of Classical plasticity was left intact after the Renaissance transformation and how strong the bonds of the intrinsic aesthetic unity were that held Renaissance composition together. It would also be interesting to see if the mathematical constants of Classical antiquity reappear in any of the relatively novel details. Finally, will Renaissance architecture reflect the same logic that convinced ancient builders to homogenize the façade's fractal dimension? We should be able to answer these questions by deciphering the specific and average values in Tables 5–8.

First, the values of linear and areal Hausdorff dimensions in Tables 5–8 meet our basic expectations, since the former are always between 1 and 2, while the latter are between 2 and 3, which suggests that our calculations are right. It can also be noticed in these tables

that the average linear dimensions grow in accordance with the relative size of the detail; that is, window jambs and lintels are more or less of the same scale, while porticoes and wall cornices are usually greater. Linear  $D_{H1}$  values are increasing exactly in this order. This reaffirms our suspicion about the Classical logic of compensation, which we first noted at the Roman Theatre of Marcellus when the enormous size of the entablature triggered a relative overdose of linear plasticity.

It is also important to add that the average  $D_{H1}$  measured at the Classical entablatures (Table 3) draws very near to that of the Renaissance wall cornices (Table 8). With a difference of less than 7%, the Renaissance interpretation of the Classical entablature as a cornice is mathematically sound, regardless of the fact that the stylistically mixed and often proportionally exaggerated Quattrocento palaces may substantially differ from the clear-cut unity of an ancient temple [23] (Book IV). Based on these observations, one could also claim that Classical plasticity is felt in Renaissance architecture even without the true continuity of Vitruvian geometry [30,33].

Following the ‘compensation rule’, we would also foretell the tendencies of areal plasticity regarding scale, but the computed values here do not seem to follow the same guidelines. However, once again we need to remember the case for the Classical frieze, where ornaments enrich otherwise empty fields with virtuosic details. This may be taken into account as a hidden factor that would hypothetically harmonize size with plasticity and set the same order as the values of  $D_{H1}$  do. One could recognize the same idea by looking at the Loggia del Commune of Brescia (Figure 7).

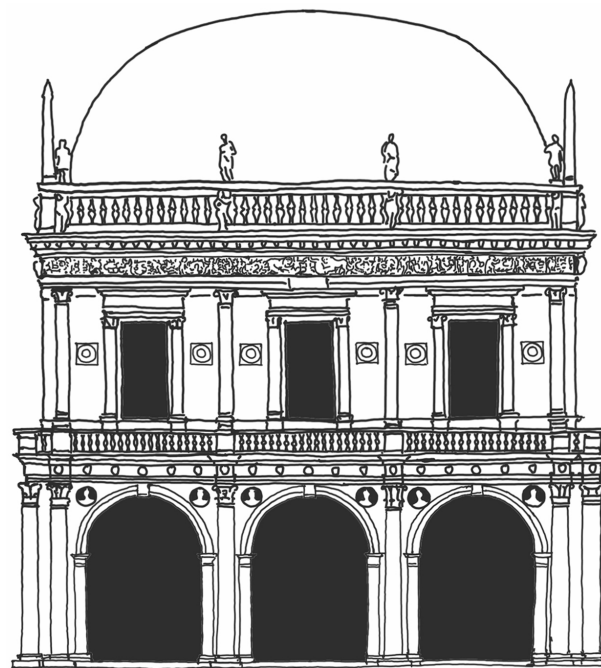


**Figure 7.** The frontage of the Loggia del Commune in Brescia (Jacopo Sansovino, 1558), illustrating the ‘compensation rule’: the lower frieze is cut into three modestly decorated parts, while the upper frieze is undivided but lavishly ornamented.

The tripartite elevation of the city hall designed by Venetian architect Jacopo Sansovino—however, there are speculations suggesting that there are connections between Bramante and the Loggia [47]—comprises two main cornices, the lower of which is divided into three parts. These parts are shorter and less ornamental than the rampant frieze of the upper cornice. It is significant that the latter cornice is also taller and undivided. This indicates that size growth will attract more ornaments, and the designer feels more comfortable if the areal plasticity ( $D_{H2}$ ) is balanced throughout the building’s frontage, hence the compensation with more details for the loss of plasticity due to size.



$D_{H2}$  values prove useful in the recognition of other intrinsic connections too. Most importantly, horizontal objects show greater coherence as the average areal dimensions of Renaissance lintels (Table 6), wall cornices (Table 8), and Classical entablatures (Table 3) have approximately the same values. The latter two are extremely close to each other, within 1%, while the average lintel differs from them by less than 3%.

The tightest liaison, however, appears between the Renaissance porticoes (Table 7) and the shafts of Classical columns (Table 2). Both being dominant and emphatic parts of the façades, they prove to play the same role in the buildup of traditional edifices. This is unambiguously shown by their areal plasticities that are equal within a 0.2% error margin and slightly above 2.35.

The coherences one can observe by the Feret diameters are also meaningful. On one hand, it is not a real surprise that the values of Classical shafts (Table 2) and that of the Renaissance jambs (Table 5) are close, since these diameters are consequences of Classical proportions, which Renaissance jambs, as miniature columns, tend to keep. This applies to the case of entablatures (Table 3) and wall cornices (Table 8) as well, where the difference is less than 1%.

The connection of these two horizontal elements is now proven, since all their Feret diameters and linear and areal Hausdorff dimensions are connected together. On the other hand, it is the least obvious why the ratio of the average Feret diameters of the horizontal ( $F_h$ ) and the vertical parts ( $F_v$ ) appear to be close to a familiar constant:

$$\frac{F_h}{F_v} \approx \pi \quad (9)$$

This applies to the ratio of the average Feret diameters of Renaissance wall cornices and jambs and that of the Classical entablatures and shafts. Rather strangely, cornices are coupled with jambs and not with porticoes, but in the case of the Feret diameters cornices are measured in relative units; scale does not have any role, only the geometrical proportions do.

We could interpret this outcome not as an arbitrary coincidence but instead as a result that might be implied by the premises of our logarithmic calculations (Equations (2) and (3)), although a more satisfying explanation is yet unfound. Temporarily, we can hypothesize that horizontal entities were more associated with round geometries; hence,  $\pi$  appears as an irrational ratio, while vertical ones were considered rational for their roles as load-bearing posts.

## 6. Limitations and Implications (Discussion)

In our previous article [1], we did not introduce any reference unit. As a result, the values of  $D_H$  in that article are slightly dependent on the randomly chosen modules, despite these modules being suggested by the tectonic layers of the evaluated façades. The current article managed to fulfil this postponed task. However, there are two further limitations and implications that need to be considered.

First, the abstract tools that this article described are not capable of measuring the additional plasticity of the frieze ornaments. To achieve this, it would be necessary to use 3D scanners and, by applying the formula in Equation (7), compare the total surface area with the area of the visible plane. If the goal were to involve planar decorations and implement complex measurements, we would need to combine various planar methods [48] with the relief method [1].

Second, when we made our last comparison between the Renaissance porticoes (Table 7) and the shafts of Classical columns (Table 2), we used the most characteristic pillar segment of a portico—or an individually composed set of shafts in a colonnade—and a single Classical column. This result has a certain poetic aspect through which we may visualize this single shaft as a ‘concentrate’ of a more complex or multilayered vertical structure. This relationship becomes even more engaging considering that we applied the Vitruvian

module as a reference unit only in case of the column. If we had not, the logarithmic result would not be much different; however, the similarity would be less conspicuous.

Our survey also allows us to understand the differences between Classical and modern architectures. Modern architecture is viewed by many scholars [13,20,22] as handling façades rather arbitrarily; since there are few ornaments or balancing tectonic layers, the fractal dimension of details may differ due to scale and architectural emphasis. This is in parallel with the differences between the static system of social values of antiquity and the ecstatic dynamism of modern industrial progress [49]. This cultural schism was recognized and duly symbolized by Robert Venturi and Denise Scott-Brown [50] (p. 106), the postmodernist designers of the National Gallery Sainsbury Wing extension in London (1991).

The future applications of the method that this article elaborated may spread from individual architectural design to complex urban analyses. Despite the general misconception about buildings' aesthetics being an arbitrary matter, we promote traditional and emerging methods [13,25,51,52] to decide if users would prefer a certain architectural design before funds were sunk into its costly construction. Rational economies should consider visual aesthetics and monitor their contribution to visual attention [53], well-being [10], and cultural complexity [49,54], which then may affect both real estate prices and human resources.

Our method may provide an interdisciplinary answer to the high street crisis of many of the historical cities in the world. Fractal analysis with improved measuring devices, such as 3D scanners, could be used for measuring the plasticity of wider tectonic structures. Further investigations could help collect data to increase the desirability of abandoned public streets [55,56]. The results presented in this article may also support urban policy makers with a mathematical tool for the conscious use of local 'pattern grammar', that is, the genius loci [16,17], for restoring and developing environments that people recognize as their own.

## 7. Conclusions

This article aimed to draw readers' attention to methodological problems regarding fractal analysis in architecture. Although our observations may be more generally applied, we focused on the tradition and historical continuity of Classical architecture, which was analyzed by this relatively novel means. More specifically, our main interest was the buildup of elevations, which we attempted to measure and categorize in order to turn visual patterns into controlled mathematical information.

The purpose of refining this information was to find implied but not obviously visible connections between the logic of Classical and Renaissance architecture. We believed that fractal analysis could point out and identify repeating patterns in a more complex manner than the common practice that evaluated planar and visual proportions only. Architecture is indeed not just visual but is also haptic; hence, we managed to introduce an evaluation method based on surface depth. This approach was published before as the 'relief method' [1], which this study extended in order to provide a more detailed survey on historical façades.

For the measurements, we used simple graphic tools and applied logarithmic Hausdorff–Besicovitch formulas to process the gained numeric data. Fractal dimensions were derived from section contours and spans, which resulted in certain linear and areal plasticity values. As a third informative component, the Feret diameter was introduced as an evaluation tool. The analyzed samples were chosen from among the best-known historical examples of the Classical antiquity and Renaissance periods, taking into account the stylistic differences in the former and the multiple functions in the latter.

Our observations were based on the average values of Feret diameters and fractal dimensions, which we interpret as the characteristic constants of the tectonic elements. With this practice, we could attribute three constants to each, which we categorized according to their scale and role in the trabeated system. These numbers and categories played major roles when comparing the haptic features of the architectural details.

Results have proved that Classical and Renaissance architectures are tied not only by formal and proportional aspects but also through similar plasticity features, even when their stylistic and geometrical premises do not match. We managed to observe a ‘compensation rule’ that portrayed the façade designs during both of the examined epochs. This regularity suggests that the ‘membrane’ of the edifice should be equally plastic; that is, the fractal dimensions of the most essential details of the building should not preferably differ. In addition, we found mathematical evidence for the palimpsest of Classical details in certain Renaissance elements based on their scale and plasticity.

Though the pure sequence of Greek and Roman columns disappears, porticoes and multilayered pillar compositions take their place in the fractal scale. In the same way, tripartite entablatures give way to cornicioni, while jambs and lintels reflect the rearrangement of ancient tectonic details more loosely. They reaffirm the ‘compensation rule’, which also implies that size growth attracts either split composition or elaborate details such as ornaments. Elevations neglecting this criterion were seen as likely inharmonious.

**Funding:** This research received no external funding.

**Data Availability Statement:** The data presented in this article is available upon request from the corresponding author.

**Acknowledgments:** I would like to thank Wolfgang E. Lorenz for his invitation and friendly support during the preparations for this publication. I also thank James Reese for proofreading. All the figures are hand-drawn by the author.

**Conflicts of Interest:** The author declares no conflict of interest involved in this article.

## References

1. Katona, V. Relief method: The analysis of architectonic façades by fractal geometry. *Buildings* **2021**, *11*, 16. [\[CrossRef\]](#)
2. Samalavicius, A. Ideology as geometry—A note on parametricism and its theoretical foundations. *Symmetry Cult. Sci.* **2020**, *31*, 353–364. [\[CrossRef\]](#)
3. Batty, M.; Longley, P. *Fractal Cities: A Geometry of Form and Function*; Academic Press: London, UK; San Diego, CA, USA, 1994.
4. Bovill, C. *Fractal Geometry in Architecture and Design*; Birkhäuser: Boston, MA, USA, 1996. [\[CrossRef\]](#)
5. Lorenz, W.E. Estimating the fractal dimension of architecture. In Proceedings of the 30th International Conference on Education and Research in Computer Aided Architectural Design in Europe—eCAADe 2012, Prague, Czech Republic, 12–14 September 2012; Volume 1, pp. 505–513.
6. Salingaros, N.A. Fractal art and architecture reduce physiological stress. *J. Biourbanism* **2012**, *2*, 11–28.
7. Ostwald, M.J.; Vaughan, J. *The Fractal Dimension of Architecture*; Birkhäuser: Cham, Switzerland, 2016. [\[CrossRef\]](#)
8. Dawes, M.J.; Ostwald, M.J.; Lee, J.H. The mathematics of ‘natural beauty’ in the architecture of Andrea Palladio and Le Corbusier: An analysis of Colin Rowe’s theory of formal complexity using fractal dimensions. *Fractal Fract.* **2023**, *7*, 139. [\[CrossRef\]](#)
9. Lorenz, W.E.; Andres, J.; Franck, G. Fractal aesthetics in architecture. *Appl. Math. Inf. Sci.* **2017**, *11*, 971–981. [\[CrossRef\]](#)
10. Taylor, R.P. Reduction of physiological stress using fractal art and architecture. *Leonardo* **2006**, *39*, 245–251. [\[CrossRef\]](#)
11. Sprott, J.C. Automatic generation of iterated function systems. *Comput. Graph.* **1994**, *18*, 417–425. [\[CrossRef\]](#)
12. Draves, S.; Abraham, R.; Viotti, P.; Abraham, F.D.; Sprott, J.C. The aesthetics and fractal dimension of electric sheep. *Int. J. Bifurcat. Chaos* **2008**, *18*, 1243–1248. [\[CrossRef\]](#)
13. Salingaros, N.A. Symmetry gives meaning to architecture. *Symmetry Cult. Sci.* **2020**, *31*, 231–260. [\[CrossRef\]](#)
14. Katona, V. Reconsidering the tectonic: On the sacred ambivalence of the tectonic in the light of Martin Heidegger and relevant theoretical studies on architecture. *Per. Pol. Architect.* **2010**, *41*, 19–25. [\[CrossRef\]](#)
15. Schumacher, T.L. The Palladio variations: On reconciling convention, parti, and space. *Cornell J. Architect.* **1987**, *3*, 12–29.
16. Katona, V.; Vukosavljević, Z. Place and identity: Critical regionalism in the new millennium, national and international achievements. *Építés-Építészettudomány* **2012**, *40*, 141–174. [\[CrossRef\]](#)
17. Norberg-Schulz, C. *Genius Loci: Towards a Phenomenology of Architecture*; Academy Editions: London, UK, 1980.
18. Vitruvius Pollio, M. *The Ten Books on Architecture*; Morgan, M.H., Translator; Dover Publications: New York, NY, USA, 1960.
19. Semper, G. Die Textile Kunst für sich betrachtet und in Beziehung zur Baukunst. In *Der Stil in Den Technischen und Tektonischen Künsten Oder Praktische Aesthetik: Ein Handbuch für Techniker, Künstler und Kunstfreunde*; Piel, F., Ed.; Mäander Kunstverlag: Mittenwald, Germany, 1977; p. 227.
20. Rowe, C.; Slutzky, R. Transparency: Literal and phenomenal. *Perspecta* **1963**, *8*, 45–54. [\[CrossRef\]](#)
21. Frampton, K. Rappel à l’ordre: The case for the tectonic. In *Theorizing a New Agenda for Architecture: An Anthology of Architectural Theory 1965–1995*; Nesbitt, K., Ed.; Princeton Architectural Press: New York, NY, USA, 1996; pp. 516–528.
22. Schumacher, T.L. The skull and the mask: The modern movement and the dilemma of the façade. *Cornell J. Architect.* **1987**, *3*, 4–11.

23. Palladio, A. *The Four Books on Architecture*; Tavernor, R.; Schofield, R., Translators; The MIT Press: Cambridge, MA, USA, 1997.
24. Wittkower, R. Alberti's approach to antiquity in architecture. *J. Warbg. Court. Inst.* **1940**, *4*, 3. [CrossRef]
25. Salingaros, N.A. Applications of the golden mean to architecture. *Symmetry Cult. Sci.* **2018**, *29*, 329–351. [CrossRef]
26. Mandelbrot, B.B. *The Fractal Geometry of Nature*; W.H. Freeman: New York, NY, USA, 1983. [CrossRef]
27. Heidegger, M. The origin of the work of art. In *Poetry, Language, Thought*; Hofstadter, A., Translator; Harper & Row: New York, NY, USA, 1971; pp. 143–162.
28. Brown, C.A.; Johnsen, W.A.; Butland, R.M.; Bryan, J. Scale-sensitive fractal analysis of turned surfaces. *CIRP Ann. Manuf. Techn.* **1996**, *45*, 515–518. [CrossRef]
29. Brown, C.A.; Johnsen, W.A.; Hult, K.M. Scale-sensitivity, fractal analysis and simulations. *Int. J. Mach. Tool. Manu.* **1998**, *38*, 633–637. [CrossRef]
30. Lefas, L. The strict and the broad sense of symmetry in Vitruvius' De Architectura. *Symmetry Cult. Sci.* **2018**, *29*, 353–363. [CrossRef]
31. Broadie, S. *Nature and Divinity in Plato's Timaeus*; Cambridge University Press: Cambridge, UK, 2012. [CrossRef]
32. Eisenman, P. The end of the Classical: The end of the beginning, the end of the end. *Perspecta* **1984**, *21*, 154–173. [CrossRef]
33. Kappraff, J. Linking the Musical Proportions of the Renaissance with the Modulor of Le Corbusier and the System of Roman Proportions. *Int. J. Space Struct.* **1996**, *11*, 211–219. [CrossRef]
34. Kappraff, J. Systems of proportion in design and architecture and their relationship to dynamical systems theory. *Symmetry: Cult. Sci.* **1999**, *10*, 299–316.
35. Déry, A. *Klasszikus Formatan*; The Canon of Classical Form; Terc: Budapest, Hungary, 2005.
36. Cauchy, A.L. Recherche sur les polyèdres—premier mémoire. *J. L'école Polytech.* **1813**, *9*, 66–86.
37. Alberti, L.B. *On the Art of Building in Ten Books*; Rykwert, J.; Tavernor, R.; Leach, N., Translators; MIT Press: Cambridge, MA, USA, 1988.
38. Vignola, G.B. *The Five Orders of Architecture*; Juglaris, T.; Locke, W., Translators; Norwood Press: Norwood, MA, USA, 1889.
39. Scamozzi, V. *The Idea of a Universal Architecture*; Garvin, P., Translator; Architectura & Natura Press: Amsterdam, The Netherlands, 2003.
40. Serlio, S. *On Architecture*; Books I–V of "Tutte l'opere d'architettura et Prospetiva"; Hart, V.; Hicks, P., Translators; Yale University Press: New Haven, CT, USA, 2005; Volume 1.
41. Summerson, J. *The Classical Language of Architecture*; MIT Press: Boston, MA, USA, 1965.
42. Boardman, J. The Parthenon Frieze: A closer look. *Rev. Archeol.* **1999**, *99*, 305–330.
43. Neils, J. *The Parthenon Frieze*; Cambridge University Press: Cambridge, UK, 2001.
44. McEwen, I.K. Symmetry takes command—The case of the Roman Capitol. *Symmetry Cult. Sci.* **2018**, *29*, 365–388. [CrossRef]
45. Calza Bini, A. Il Teatro di Marcello. *Boll. Cent. Studi Stor. Archit.* **1953**, *7*, 1–43.
46. Fidenzoni, P. *Il Teatro di Marcello*; Liber: Rome, Italy, 1970.
47. Hemsoll, D. Bramante and the Palazzo della Loggia in Brescia. *Arte Lomb.* **1988**, *86–87*, 167–179.
48. Lorenz, W.E.; Kulcke, M. Multilayered complexity analysis in architectural design: Two measurement methods evaluating self-similarity and complexity. *Fractal Fract.* **2021**, *5*, 244. [CrossRef]
49. Frampton, K. Towards a critical regionalism: Six points for an architecture of resistance. In *The Anti-Aesthetic: Essays on Postmodern Culture*; Foster, H., Ed.; Bay Press: Port Townsend, WA, USA, 1983; pp. 16–30.
50. Venturi, R.; Scott Brown, D.; Izenour, S. *Lerning from Las Vegas: The Forgotten Symbolism of Architectural Form*; MIT Press: Cambridge, MA, USA, 1977.
51. Gruson, F. The spirit and the symbol in architecture—The divine proportion. *Symmetry Cult. Sci.* **2019**, *30*, 5–14. [CrossRef]
52. Mehaffy, M.W.; Salingaros, N.A. Symmetry in architecture—Toward an overdue reassessment. *Symmetry Cult. Sci.* **2021**, *32*, 311–343. [CrossRef]
53. Lavdas, A.A.; Salingaros, N.A. Architectural beauty: Measurable and objective. *Challenges* **2022**, *13*, 56. [CrossRef]
54. Norberg-Schulz, C. The phenomenon of place. In *Theorizing a New Agenda for Architecture: An Anthology of Architectural Theory 1965–1995*; Nesbitt, K., Ed.; Princeton Architectural Press: New York, NY, USA, 1996; pp. 414–428.
55. Office for National Statistics (UK). High Streets in Great Britain: March, 2020 [Official Release]; 2020. Available online: <https://www.ons.gov.uk/peoplepopulationandcommunity/populationandmigration/populationestimates/articles/highstreetsingreatbritain/march2020> (accessed on 18 February 2023).
56. Akbarishahabi, L. Evaluating the relationship between fractality and imageability principles for sustainable urbanism: An experimental study. In *Research & Reviews in Architecture, Planning and Design*; Parlak Bicer, Z.O., Gürani, F.Y., Eds.; Gece Kitaplığı: Ekim, Turkey, 2022; pp. 37–57.

**Disclaimer/Publisher's Note:** The statements, opinions and data contained in all publications are solely those of the individual author(s) and contributor(s) and not of MDPI and/or the editor(s). MDPI and/or the editor(s) disclaim responsibility for any injury to people or property resulting from any ideas, methods, instructions or products referred to in the content.